nature ecology & evolution

ARTICLES

PUBLISHED: 4 JANUARY 2017 | VOLUME: 1 | ARTICLE NUMBER: 0016

Coupling phenotypic persistence to DNA damage increases genetic diversity in severe stress

Gilad Yaakov*‡, David Lerner‡, Kajetan Bentele†‡, Joseph Steinberger† and Naama Barkai*

Mutation rate balances the need to protect genome integrity with the advantage of evolutionary innovations. Microorganisms increase their mutation rate when stressed, perhaps addressing the growing need for evolutionary innovation. Such a strategy, however, is only beneficial under moderate stresses that allow cells to divide and realize their mutagenic potential. In contrast, severe stresses rapidly kill the majority of the population with the exception of a small minority of cells that are in a phenotypically distinct state termed persistence. Although persisters were discovered many decades ago, the stochastic event triggering persistence is poorly understood. We report that spontaneous DNA damage triggers persistence in *Saccharomyces cerevisiae* by activating the general stress response, providing protection against a range of harsh stress and drug environments. We further show that the persister subpopulation carries an increased load of genetic variants in the form of insertions, deletions or large structural variations, which are unrelated to their stress survival. This coupling of DNA damage to phenotypic persistence may increase genetic diversity specifically in severe stress conditions, where diversity is beneficial but the ability to generate *de novo* mutations is limited.

Phenotypic persisters are individual microbes that survive harsh treatments that kill the majority of their genetically identical sister cells[1–11]. Persistence has been described in many bacterial species, and was recently implicated in the ability of individual cancer cells to survive chemotherapy[12,13]. Revealing the stochastic event triggering persistence is a major challenge to eradicating this subpopulation. Drug persistence has not been described in budding yeast, but a small fraction of cells have been shown to survive harsh environmental stresses[14–16]. While survivors are always expected, we observed a clear signature of persistence when subjecting cells to the antifungal drug fluphenazine: following the initial rapid exponential decline in the fraction of living cells, death rate was significantly reduced, indicating a small subpopulation (~10^{-3}) of persisters (Fig. 1a).

A molecular marker for yeast persisters

To uncover events that trigger cells to become persisters, we established a marker to detect persisters in the rapidly growing, unstressed population. Since increased stress survival has been linked to stochastic activation of stress genes[15,16], we asked whether heat-shock protein 12 (Hsp12) may serve as such a marker. Hsp12 is strongly induced by a variety of environmental stresses[17] and its levels fluctuate highly between individual cells, with a subset of cells reaching high levels characteristic of stress-exposed cells (Fig. 1b).

We examined whether high Hsp12 expression predicts stress survival by sorting single cells expressing either high (top 0.1%, termed 'extreme') or normal (the remaining 99.9%, termed 'control') Hsp12-GFP (green fluorescent protein) into 96-well plates (Fig. 1c), and monitoring their ability to survive and generate a colony in a range of harsh stresses. In unstressed conditions, cells expressing extreme Hsp12 levels survived less well than control cells. In sharp contrast, extreme cells better survived practically all stress exposures (Fig. 1d,e). To verify that extreme cells maintain their advantage under competitive conditions, we co-sorted differentially labelled extreme and control cells into the same well at different initial frequencies, and measured the relative fraction of their progenies at saturation. This was made possible by sorting Hsp12-mCherry extreme and control cells from GFP-labelled or GFP-negative co-cultured strains. As stress levels rose, extreme cells became increasingly successful in out-competing control cells (Fig. 1f). For example, extreme frequency increased by 100-fold, from ~0.1% to ~10%, after sorting into media containing 1.7 M NaCl. Cultures seeded from a sorted extreme cell lost their high Hsp12 levels (Fig. 1g) and showed normal stress sensitivity, confirming that these cells are indeed phenotypic persisters. We conclude that Hsp12 marks budding yeast persisters.

Prolonged DNA damage leads to yeast persisters

To better understand the phenotype of extreme Hsp12-expressing cells, we sorted the cells using fluorescence-activated cell sorting (FACS) and imaged them using microfluidics-coupled video microscopy. About half (59%) of the sorted cells were large budded, resembling DNA damaged cells that are checkpoint-arrested at metaphase[18,19]. To examine whether Hsp12 induction correlates with DNA damage, we fluorescently tagged Rad52, a nuclear protein that localizes to positions of DNA double-strand breaks (DSB)[20,21], confirming that approximately half of the sorted extreme cells had a long-lived (>40 min) Rad52 focus, while almost no control cells had such a focus (Fig. 2a). When subjecting these sorted cells to the antifungal drug fluphenazine, the focus-containing, high Hsp12-GFP cells better survived (Fig. 2b). About half of the focus-containing surviving cells resumed normal growth following drug treatment, while the rest did not divide robustly (Fig. 2b and Supplementary Fig. 1a). Diploid cells grew better than haploids, possibly due to a higher capacity to repair DNA damage from the undamaged locus. Therefore, extreme cells portray morphology and markers associated with prolonged DNA damage.

To examine whether Hsp12 induction follows DNA damage, we imaged freely cycling cells carrying Hsp12-mCherry and Rad52-GFP

Department of Molecular Genetics, Weizmann Institute of Science, Rehovot 76100, Israel. †Present addresses: Core Unit Bioinformatics, Berlin Institute of Health, Berlin 10117, Germany (K.B.); Department of Physiology and Biophysics, Weill Cornell Medical College, New York, New York 10021, USA (J.S.). ‡These authors contributed equally to this work. *e-mail: gilad.yaakov@weizmann.ac.il; naama.barkai@weizmann.ac.il

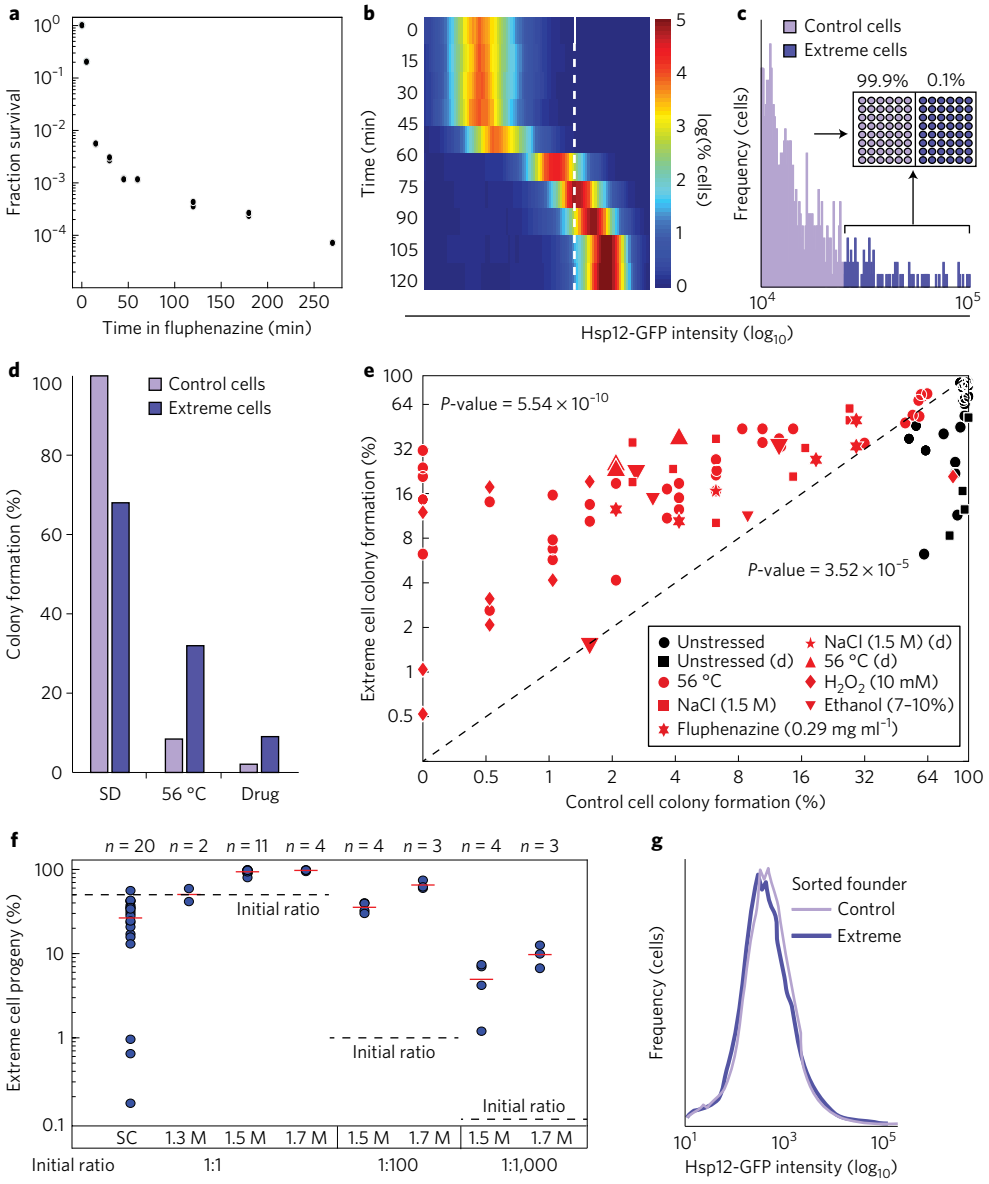

Figure 1 | Hsp12 is a marker of budding yeast persisters. a, The fraction of cells that survived exposure to fluphenazine for the indicated times. Duplicates are plotted separately. **b**, Distributions of Hsp12-GFP fluorescence in cells exposed to 0.9 M NaCl. *y* axis: exposure times; *x* axis: fluorescence intensity. Cell frequency is colour coded. The white line denotes the border of extreme cells pre-stress. **c**–**e**, Hsp12 extreme cells better survive drug exposure. **c**, Scheme of the experiment. **d**, Fraction of extreme or control sorted cells that formed a visible colony in representative experiments. SD: unstressed; 56 °C: 20 min heat-shock; drug: fluphenazine. **e**, Summary of all experiments. Each dot is one plate, and is plotted for its fraction of sorted extreme versus control cells that formed a colony. Symbols correspond to different conditions (for EtOH, a larger symbol corresponds to higher % EtOH). Cells were haploid unless specified (d = diploid). *P*-values are based on paired *t*-test. **f**, Fraction of extreme cell progeny in saturated cultures, following their co-culturing and co-sorting with control cells at the initial ratio indicated by dotted lines. Each point represents one experiment, with their mean denoted by a red line. Number of repeats is indicated on top. **g**, Distributions of Hsp12-GFP expression in cultures generated from single sorted extremes and control cells.

(Supplementary Video 1). Appearance of a Rad52 focus was the first indication of DNA damage, followed by cell-cycle arrest and Hsp12 induction (Fig. 2c,d and Supplementary Fig. 1b). After ~3–5 h of arrest, cells re-entered the cell cycle, either losing the Rad52 focus and resuming normal division time (~60% of cells), or maintaining the focus and entering a second arrest (Fig. 2e and Supplementary Fig. 1b). Hsp12 began to dilute once cells resumed division (Fig. 2c and Supplementary Fig. 1b). Exposing these cells to a high dose of fluphenazine led to the rapid killing of most cells, with a minority of survivors, many of which were DNA-damaged, high Hsp12-expressing cells (Supplementary Fig. 2 and Supplementary Videos 2 and 3). This same dynamic was confirmed with a second marker of DNA damage, Rnr3 (refs [22,23]), whose induction also preceded Hsp12 induction and predicted drug survival (Supplementary Fig. 3 and Supplementary Video 4).

Consistent with the idea that DNA damage triggers persistence, we find an increased fraction of persisters in strains showing elevated mutation rates, as indicated by higher fractions of extreme Hsp12-expressing cells with increased stress survival (Supplementary Fig. 4). To verify directly that DNA damage triggers persistence, we induced DSBs by expressing a GAL1-inducible HO (homothallic switching) endonuclease in cells with a single HO cleavage site. Inducing HO led to the appearance of Rad52-GFP foci, followed by a delayed (~2 h) induction of

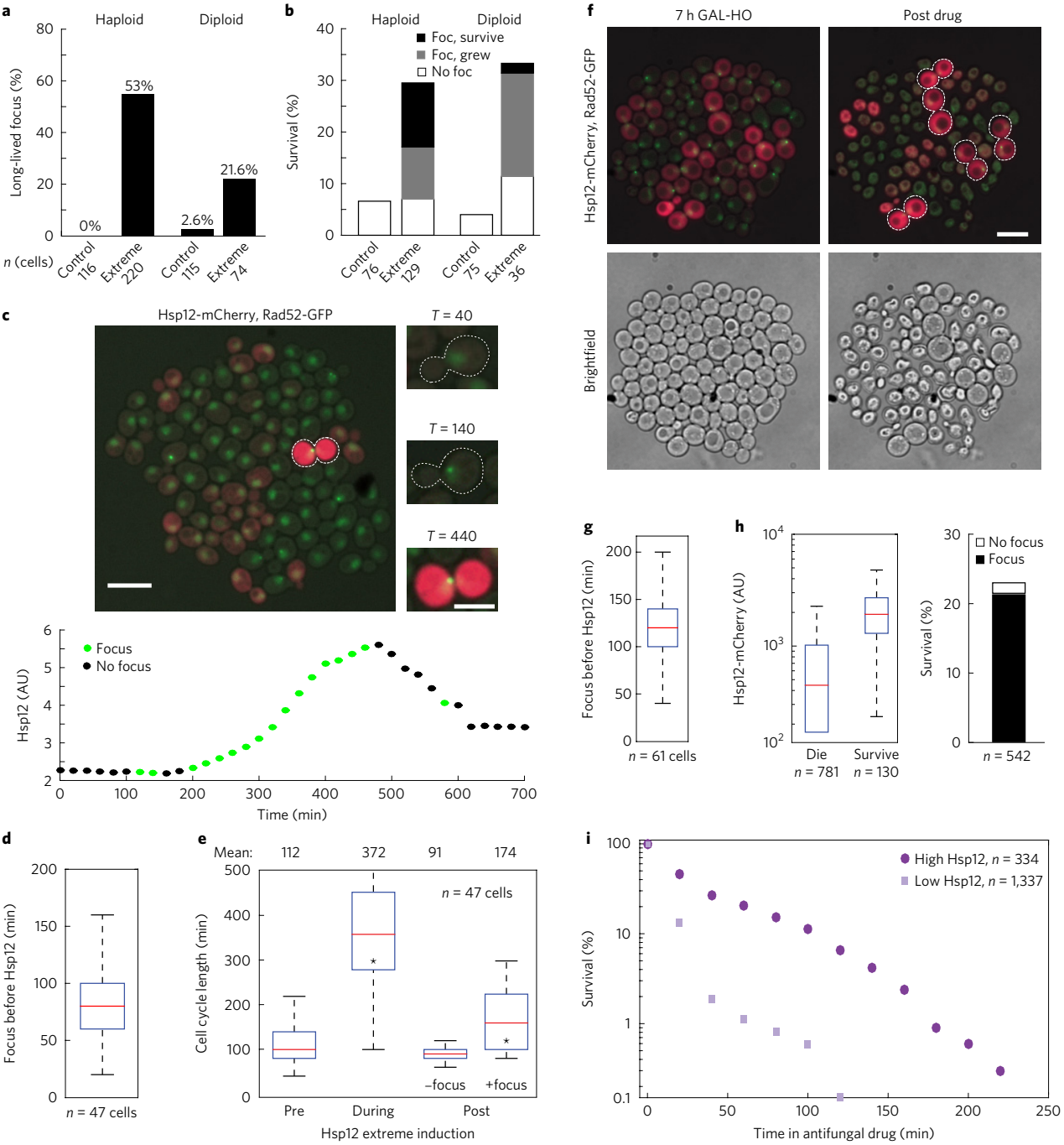

Figure 2 | DNA damage leads to yeast persisters. a,**b**, Hsp12 extreme cells show DNA damage markers and better survive drug exposure. Haploid and diploid FACS-sorted cells were transferred to a microfluidics chamber, imaged, and subjected to a pulse of fluphenazine. Fractions of cells with stable (>40 min) Rad5-GFP foci (**a**), and survivors (**b**) are shown. Foc, focus. Survivors were classified based on presence of a focus, and resumption of proliferation following drug treatment (grew), or survival without dividing >2 in 15 h after drug removal (survive) (Supplementary Fig. 1a). **c**–**e**, Hsp12 is induced following DNA damage and cell cycle arrest. **c**, Representative extreme Hsp12-mCherry expressing cell; scale bar, 10 µm (Supplementary Video 1). Focus appearance and Hsp12-mCherry induction in this cell, outlined with dashed white line (scale bar, 5 µm) and quantification with green dots indicating a Rad52-GFP focus are shown. **d**,**e**, Boxplots (25–75 percentile in the box, median in red and 2.7σ tails) show the distribution of time delays between focus appearance and Hsp12 induction (**d**), and the cell division times before, during and after Hsp12 induction (**e**). Forty-seven cells with a stable (>80 min) focus were analysed. Division time is measured between two subsequent anaphases. Cells that resolved (63%) or maintained the focus before re-entering the cell cycle (see Supplementary Fig. 1b) were distinguished. Forty percent of cells that retained the focus didn't complete the subsequent division during the movie, leading to an underestimate (asterisks). **f**–**i**, DSB induction triggers Rad52 foci, Hsp12 expression and drug survival. Single cells were grown into microcolonies for 7 h in non-inducing raffinose, after which GAL-HO was induced for 7 h with galactose, leading to stable Rad52 foci in 50.4% of 542 cells, versus 3% of 846 cells grown in parallel without HO (Supplementary Fig. 5). Fluphenazine was pulsed in and survival scored. **f**, A representative image before and after drug exposure with circles outlining survivors (scale bar, 10 µm; Supplementary Videos 5 and 6). **g**, Hsp12 induction followed Rad52 focus appearance with ~2 h delay. **h**, Practically all drug survivors had a stable focus (>1 h) and expressed high Hsp12 levels before the exposure. **i**, The rate of cell death from a constant drug exposure, distinguishing cells expressing the top 20% (High Hsp12) before drug exposure from the rest of the population (Low Hsp12).

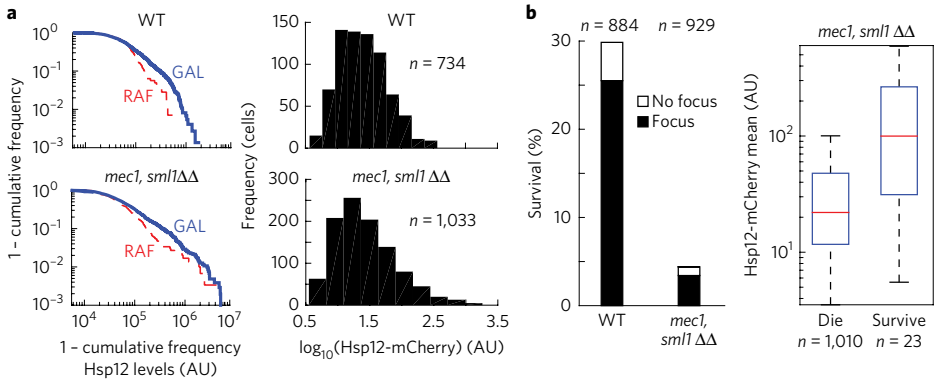

Figure 3 | Drug persistence depends on an intact DNA damage checkpoint. a,**b**, Cells expressing the GAL–HO endonuclease were grown as in Fig. 2f. 37.2% of *mec1*,*sml1* double-deleted cells had a stable Rad52 focus after 7 h of HO induction, compared with 30.5% of WT. Hsp12 levels increased, shown by the shift in the histograms comparing cells before and after HO induction (**a**). 1 – cumulative frequency is the probability that Hsp12 levels are above the given value. Final Hsp12 levels just before drug treatment are shown on the right. The fraction of drug survivors was reduced in *mec1*, although the surviving cells expressed higher Hsp12 levels compared with the control (**b**), shown in boxplots as in Fig. 2d.

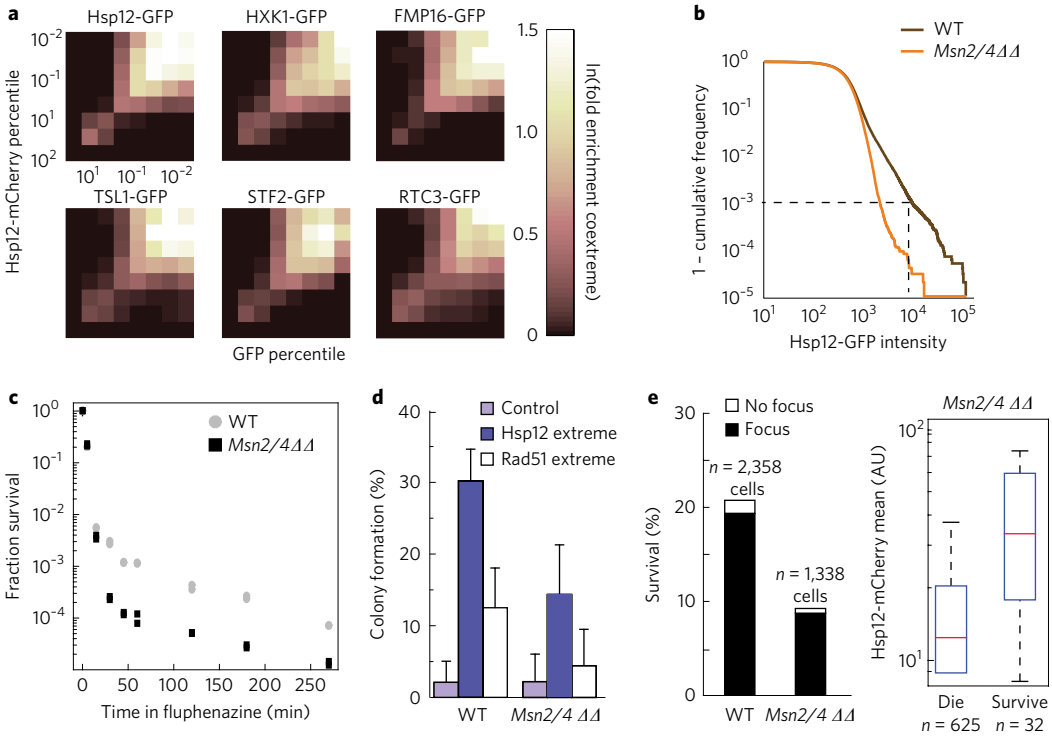

Figure 4 | Activation of the general stress response is important for yeast persistence. a, Log-phase diploids expressing Hsp12-mCherry and the indicated GFP-labelled stress gene were analysed by flow cytometry. Co-induction was measured by fold enrichment in cells showing GFP and mCherry fluorescence above two respective percentiles. Co-enrichment matrices demonstrate that Hsp12 extremes are also extreme for the indicated stress genes. Not all stress genes analysed were part of this co-extreme group (Supplementary Fig. 8a). **b**, Cumulative single cell distribution of Hsp12-GFP expression in wild-type and *Msn2/4ΔΔ* strains. The dotted line denotes the top 0.1% expressing cells. **c**, *Msn2/4ΔΔ* cultures were exposed to fluphenazine for the indicated times, and survival was scored. WT results are from Fig. 1a, shown for comparison. Duplicates are plotted separately for each strain. **d**, Wild-type and *Msn2/4ΔΔ* cells were sorted for control or extreme levels of Hsp12, or control or extreme levels of the *Msn2/4*-independent DNA damage response gene *Rad51* (Supplementary Fig. 8b). Sorted cells were assayed for survival in 1.5 M NaCl as in Fig. 1c,d. Error bars indicate standard of deviation. **e**, *Msn2/4ΔΔ* cells expressing GAL–HO were assayed as in Fig. 2f. The fraction of cells expressing Rad52-GFP foci following 7 h HO induction in *Msn2/4* delete was 22% versus 19% in wild type, but the mutant's drug survival was reduced. Practically all surviving cells had a focus, and expressed higher Hsp12-mCherry levels before drug exposure.

Hsp12-mCherry (Fig. 2f,g and Supplementary Fig. 5). Subjecting cells to fluphenazine confirmed that cells became persisters (Fig. 2h and Supplementary Videos 5 and 6). While ~99% of cells with low Hsp12 died within 60 min of exposure, only 25% of high Hsp12 cells died at that time, with survivors losing viability at a significantly lower rate (Fig. 2i). Nearly all survivors had Rad52 foci (Fig. 2h). We conclude that a severe DNA damage, such as DSB, triggers persistence in budding yeast.

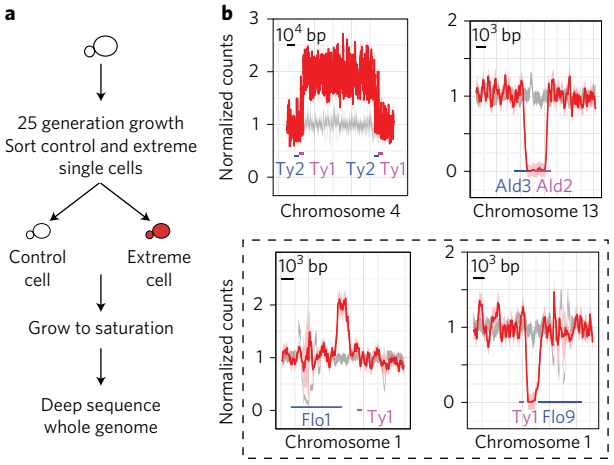

Figure 5 | Extreme cells are enriched for genetic mutations. a, A scheme of cell growth and sorting leading to whole genome sequencing. **b**, Part of the structural variations identified in the genome sequencing are plotted by comparing the normalized read count in the mutated sample (red) with the background levels (grey). The SVs in Flo1 and Flo9 (bottom) are counted only once since they are found in the same sample and likely originated from the same event.

Yeast persistence depends on checkpoint and ESR activation

The DNA damage checkpoint orchestrates the response to DNA damage. We asked whether Hsp12 induction depends on checkpoint activation. HO induction of DSBs in cells deleted of the checkpoint sensor *mec1* does not arrest the cell cycle[20,21] (Supplementary Fig. 6a), but did induce Rad52-GFP foci and Hsp12-mCherry expression (Fig. 3a). Flow cytometry analysis further indicated a higher fraction of extreme Hsp12 cells in the *mec1*-deleted strain, and in a strain deleted of the Rad53 checkpoint kinase, suggesting that this induction is not checkpoint dependent (Supplementary Fig. 6b,c). Notably, extreme cells in these checkpoint mutants did not survive drug exposure when analysed in the HO-induced system or as freely cycling cells (Fig. 3b and Supplementary Fig. 6d). This suggests that persisters better survive drug exposure because they are non-dividing, as implicated in bacteria[2–11]. Arresting cells at the end of G1 using α-factor, however, did not increase survival to fluphenazine (Supplementary Fig. 7). We therefore attribute the reduced drug survival of checkpoint-deficient mutants to their inability to repair the inflicted DNA damage, rather than the lack of cell cycle arrest.

Hsp12 is part of the environmental stress response (ESR), whose induction by a given moderate stress protects cells from a range of severe stresses[24]. ESR induction in extreme cells could therefore explain their persistence. Indeed, extreme expression of Hsp12 is regulated in *trans*, and Hsp12 extreme expression reflects a broader ESR induction, as indicated by high co-expression of a subset of ESR genes (Fig. 4a and Supplementary Fig. 8a). Furthermore, deletion of the ESR regulators, Msn2/4 (ref. [17]) strongly reduced the extreme subpopulation (Fig. 4b) and reduced stress survival in freely cycling populations (Fig. 4c). Stress persistence was also reduced in Msn2/4 DNA-damaged extreme cells, as verified by FACS based on an Msn2/4-independent DNA-damage marker (Fig. 4d and Supplementary Fig. 8b) and by HO induction of DSBs (Fig. 4e). Unexpectedly, the remaining drug survivors on *Msn2/4* deletion still expressed relatively high levels of Hsp12 (Fig. 4d,e), suggesting activation through a parallel pathway such as Hsf1. We conclude that ESR activation in extreme cells contributes significantly to their increased stress survival.

Yeast persisters are enriched for mutations

Imprecise repair of DNA damage is a major source of genetic mutations. We therefore hypothesized that the prolonged DNA damage leading to persistence might culminate in mutations. Since in exponentially growing cells about half of the mutations arise in just the last generation, we predicted that persister cells will be enriched for random mutations, unrelated to their stress survival. To examine this, we sorted and grew a total of 412 extreme and 315 control cells for deep genomic sequencing in three independent experiments (Fig. 5a). Single and multi-nucleotide polymorphisms (SNPs and MNPs), insertions or deletions (1–45 bp, indels), and large structural variations (SVs) were identified using a bioinformatics pipeline based on established software, followed by filtering, manual curation and extensive verifications by Sanger sequencing (Methods and Supplementary Information).

Indels or SVs were found in 26 of the 412 extreme samples, compared with 6 out of the 315 control samples (Table 1). By Fisher's

Table 1 | Summary of mutations detected in control and extreme cells.

	Mutated cells %	Control vs extreme *P*-value	Estimated mutation rate (per site per division)		
			Literature rates	This study	
				All divisions	Extreme divisions
SNPs					
Control	14.6 (46/315)	0.064	3.3×10^{-10}	4.9×10^{-10}	
Extreme	19.2 (79/412)			6.4×10^{-10}	5.3×10^{-9}
Small indels					
Control	1.3 (4/315)	0.017	2×10^{-11}	4.2×10^{-11}	
Extreme	4.1 (17/412)			1.4×10^{-10}	2.5×10^{-9}
SVs					
Control	0.6 (2/315)	0.079	8.3×10^{-12}	2.1×10^{-11}	
Extreme	2.2 (9/412)			7.3×10^{-11}	1.4×10^{-9}
Indels + SV					
Control	1.9 (6/315)	0.0027			
Extreme	6.3 (26/412)				

The numbers of mutated cells in each category, with the associated Fischer's test *P*-values, are summarized. Literature mutation rates[25,27] are shown for comparison with the rates calculated for control and extreme cells in this study. For extreme cells both lower and upper bounds are provided, assuming that they differ from the control cells in all divisions leading up to sorting (lower), or only the last prolonged cycle where they experienced the DNA damage (upper bound). SV, structual variation; Indels, insertion/deletions.

exact test, this enrichment is significant ($P=0.0027$). Analysed individually, we find a 3-fold enrichment of indels ($P=0.017$), ~3.5-fold enrichment of SVs ($P=0.079$) and 30% more SNPs ($P=0.064$) in extreme versus control cells. Rates for all three mutation categories were higher in extreme cells in each of the three independent experiments we performed (Supplementary Information). All detected SVs were flanked by repetitive sequences (Fig. 5b and Supplementary Information).

The frequencies of mutations in our control samples are consistent with literature values (Table 1 and Supplementary Information)[25–27]. Estimating the mutation frequency of extreme cells is less straightforward, since cells are extreme only transiently, and their division time, while being extreme, is greatly prolonged (Fig. 2e). Lower and upper bounds are obtained, however, by respectively assuming that extreme samples differ from the control cells in all 23–25 divisions, or that they differ in only the last extreme division (Table 1). The extreme dynamics we describe suggest that this mutation frequency is closer to the upper bound, namely that a division which triggers cells to become extreme has ~5% chance of generating an indel or an SV.

The molecular underpinning of persistence has proven tricky to define, partly because there may be multiple sources that render cells stress persistent. We show here that in budding yeast, strong DNA damage triggers phenotypic persistence. We propose that this coupling increases the probability that an emerging indel or SV will become fixated in the population specifically in severe stress conditions, where being a persister provides a significant survival advantage. This could help cells to better adapt to novel unexpected environments that demand unpredictable genetic changes. Phenotypic persistence is typically viewed as a bet-hedging strategy, increasing population fitness under fluctuating environments. Our study suggests a complementary outcome of increasing genetic diversity under extreme stress conditions.

Methods

Strains. Strains were constructed on verified clones from the BY4741 GFP yeast collection[28]. Diploids were generated by mating the BY4741 strain with BY4742. Standard gene deletion and tagging procedures were used[29]. *mec1* and *rad53* mutants also carry the suppressor *sml1* deletion.

All HO nuclease strains are derivatives of JKM179 (ref. [30]), which contains an HO cleavage site at the endogenous mating locus, and an integrated HO nuclease under the control of the inducible GAL1 promoter.

Growth conditions. Cells were grown in standard synthetic complete media with 2% glucose (SD). For FACS analysis and microscopy, serial dilutions were inoculated, and cultures that grew to log phase at 30 °C with a maximal optical density (OD) 0.2 were assayed the next day. We noted that the Hsp12 FACS profiles of cultures with a higher OD occasionally shifts to a higher mean. When this occurred during an experiment, the culture was replaced with a lower OD sample from the dilution series.

Liquid cultures of cells bearing the GAL-inducible HO system were grown in synthetic complete medium supplemented with 0.1% glucose and 2% raffinose. HO induction was carried out with medium containing 0.1% glucose, 2% raffinose and 2% galactose for 7 h before fluphenazine treatment. For cell cycle synchronization in G1, cells were treated with 5 μg ml^{-1} α-factor for 3 h and then challenged with fluphenazine.

FACS analysis, sorting, single-cell stress-survival experiments. Populations were monitored using BD FACSAria and BD FACSAria Fusion cell sorters. Gating was done for single cells based on the FSC-A and SSC-A counts, which are associated with cell size and geometry. GFP or mCherry levels for gated cells were then monitored versus their FSC-A level. In every experiment, 100,000 cells were analysed to obtain Hsp12 levels in the population, and the fluorescence of the 0.1% highest Hsp12 levels were used as the cutoff for extreme cells. For the mutator strains, a wild type culture analysed in parallel was used to determine the cutoff intensity for the 'wt extremes', and 'internal extremes' were calculated internally as the top 0.1% in the mutator population. Enrichment of 'wt extreme' cells in mutator strains was calculated as the percent of cells in the mutator population with Hsp12 levels higher than the extreme cell cutoff measured in the parallel wild type culture. When multiple wild type and mutator populations were measured the same day, the average of the wild type and mutator Hsp12 intensities were used.

Single cells were sorted into 96-well plates with SD media using the 'single cell' FACS sorting accuracy setting. Sorting efficiency was very high, as judged by colony growth in nearly all wells into which a single control cell was sorted (Fig. 1d,e). In over 90% of the wells that had growth, only a single colony was observed. The minority of cases where more than one colony grew from the single cell were ignored and subtracted from the total number of wells.

Cells were sorted row by row, each row consisting of half control cells (up to 99.9% Hsp12 levels) and half extreme cells. Cells were sorted into SD media and incubated at 30 °C for unstressed conditions, or sorted directly into SD supplemented with 0.29 mg ml^{-1} of water-dissolved fluphenazine dihydrochloride (Sigma F4765), 1.5 M NaCl or 7–10% EtOH. The cells were grown in the above medium, and colonies were counted after 3–4 d for unstressed conditions, and 6–7 d for stress conditions. Stress experiments were always carried out in parallel to unstressed conditions to control for sorting accuracy and efficiency.

For heat-shock pulses, plates were preheated in an incubator to 56 °C for 15 min and then placed on the preheated sorting platform. Cells were sorted into the preheated plates (4–5 min sorting time) and then returned to the 56 °C incubator for a total of 20 min from the beginning of the sorting. Following the 20 min heat shock, plates were incubated at 30 °C and colonies were counted after 3–4 d.

FACS competition experiments. The Hsp12-mcherry haploid (MATα) strain was crossed with BY4741 (GFP negative) or a BY4741 strain with the highly expressed constitutive *Tdh3* gene C-terminally tagged with GFP (GFP positive). GFP positive and negative strains were inoculated and grown in the same tube for FACS analysis and sorting. Single-cell sorting precision was used to sort GFP positive, Hsp12-mCherry extreme cells, together with GFP negative, Hsp12-mCherry control cells. As a control, extreme cells were GFP positive and control cells were GFP negative in approximately half the experiments, and vice versa in the other half.

One hundred extreme cells and 100 control cells were sorted from the same culture into a single well of a 96-well plate for competition assays between equal amounts of initial extreme and control cells (Fig. 1g). The 200 cells were sorted directly into SD media or SD with the specified stress. The volume of sorted liquid is negligible (immeasurable) for 200 cells, leaving the final stress concentration unchanged. One hundred extreme cells and 10,000 or 100,000 control cells (for initial ratios of 1:100 or 1:1,000, respectively) were sorted into 15 ml tubes, after which the final volume was measured, and the stress was uniformly applied by adding NaCl to the indicated final concentration (Fig. 1g).

The sorted cells were incubated in a shaker at 30 °C until saturation. At least 10,000 cells were then FACS analysed, and GFP positive and negative cells were readily distinguished to measure the fraction of cells originating from extreme cells versus cells originating from control cells in the final population.

Microfluidics. The CellASIC ONIX Microfluidic Platform was used as per manufacturer instructions. Y04C and Y04D microfluidic plates were utilized for haploid and diploid cells, respectively. SD was supplemented with 10% polyethylene glycol (SD-PEG) MW 3,350 to increase the viscosity and minimize cell movement from the microfluidic flow. For fluphenazine killing experiments, SD-PEG (or raffinose-based SC for HO experiments) supplemented with 1.5–1.7 mg ml^{-1} fluphenazine was pulsed in for 30–45 min, followed by fluphenazine-free media to confirm viability. Strains and treatments that were directly compared with each other were imaged in parallel chambers and conditions in the same microfluidic device.

Microscopy and image analysis. Growth of microcolonies was observed with widefield fluorescence time-lapse microscopy at 27 °C using an Olympus IX81-ZDC inverted microscope with a motorized stage (Prior). Image sets were acquired with a Hamamatsu Back-thinned ORCA-II-BT or QIMAGING Retiga R6 CCD (charge-coupled device) cameras. Fluorescent proteins were excited using EXFO X-Cite light source and Chroma 49002ET-GFP and 49008ET-mCherry filter sets. Images were acquired with 20 min intervals.

Analysis was performed using ImageJ and FIJI software and plugins, together with a macro for segmenting cells of microcolonies at the time point preceding the addition of fluphenazine. Segmentation was carried out on brightfield images of yeast slightly out of focus, so that their contour is highlighted in black. Briefly, the macro created boundaries by inverting the image, enhancing boundaries using a band-pass filter, and applying a threshold. Boundaries were then closed by two dilate and erode rounds, and segments were created by inverting the image and applying watershed. Inaccurate and unsegmented cells were then corrected and segmented manually.

Segmentation was used to analyse mean Hsp12 levels in GAL–HO induced cells directly before fluphenazine treatment. The segments were applied to the fluorescent images in which a rolling ball with a radius of 50 pixels was used to subtract the background. For measuring % survival and % foci in microcolonies after GAL–HO induction, nuclei were counted to calculate the number of cells, and foci were scored manually, only if present at least two consecutive time points (40 min). For cell survival analysis, cell death following addition of fluphenazine was readily detected by cell bursting. Cell viability of cells that did not burst was confirmed by subsequent growth in SD free of the drug, except for the experiment in which cell death was monitored as a function of time in continuous fluphenazine.

Analysis of growth dynamics of unperturbed cells that experienced a long-lasting Rad52 focus that lead to extreme Hsp12 induction were

performed manually. Cells were segmented and tracked over many divisions before, during and after the Rad52 focus and Hsp12 induction, and their size, Hsp12-mCherry levels, presence of Rad52-GFP foci and anaphase events (using the Rad52-GFP nuclear signal) were scored.

Bulk fluphenazine survival assays. An overnight culture was diluted in SD to an OD of 0.05, grown to OD 0.25, and subjected to 0.5 mg ml^{-1} fluphenazine. At the indicated times, 1 ml samples were extracted, spun down at 17,000×*g*, 900 µl were removed and replenished with fresh SD. Tenfold serial dilutions were prepared, and 100 µl of the dilutions were plated in duplicate on SD plates and incubated at 30 °C for 2 d. Plates with 100–500 colonies were counted, their dilution factor was taken into account and the final % survival was calculated by using the number of colonies before drug addition (time 0) as total cell survival. There was no cell division during the course of the experiment as verified by counting cells using a hemocytometer at time points 0, 60, 120 and 270.

Diploids co-expression analysis. Diploid cells were mCherry-tagged at the Hsp12 locus and GFP tagged the indicated locus. To define the extent of co-expression, 100,000 cells were analysed by flow cytometry. The resulting two-dimensional (GFP and mCherry) single-cell distributions of fluorescence levels were analysed as follows. Fluorescence levels were binned by the cumulative distribution fractions so that the first bin (1,1) included all cells, the bin (2,2) included the 30% of the cells with highest expression in both GFP and mCherry, the bin (2,3) included the cells with 30% highest GPF and 10% highest mCherry, and so on. The fraction of cells within each bin f_{ij} was then calculated. This fraction was then normalized by the expected fraction, assuming no correlation between GFP and mCherry expression. The generated matrix was then corrected for cell size, by repeating the procedure above, this time considering coordination between GFP (or mCherry) versus FSC-W.

Selecting extreme and control cells for sequencing. A total of three sequencing experiments were carried out. Cells were struck out on a YPD plate, and a small single colony was inoculated in 5 ml of liquid SD for a total of 46 h. The cell density of the sorted culture was measured using a hemocytometer, and the colony founder cell was calculated to undergo 25, 24 and 23 generations (for experiments 1, 2 and 3, respectively) with a doubling time of ~110 min until sorting began. This culture was FACS sorted into single control and extreme cells, which were grown to saturation in 1.5 ml. Note that if a mutation occurred after the sorted single cell divided, it would be present in only half the cells after one division, one quarter after two division, and so on, and the fraction of reads with mutations would decrease exponentially with divisions. Therefore, as we detect the mutations in most of the reads, the mutations must have occurred in the original sorted cell.

Library preparation. For library preparation, DNA was extracted by blending the cells in 300 µl lysis buffer (50 mM HEPEs pH 7.5, 140 mM NaCl, 1 mM EDTA, 1% TritonX-100, 0.1% sodium deoxycholate) with 0.5 mm zirconium oxide beads in a Bullet Blender 24 (Next Advance) for 1 min at level 8. Cleared lysate was sonicated for 20 min (0.5 s on, 0.5 s off) in a Bioeruptor plus (Diagenode) cooled water bath sonicator, resulting in an average DNA fragment size of ~300 bp. Lysates were RNAse treated for 1 h at 37 °C, and then proteinase K treated for an additional 2 h at 37 °C. From each sample, 10 µl of the lysate was taken and a multiplexed library was prepared for sequencing[31]. Libraries were sequenced in an Illumina HiSeq 2500 with 100 bp paired-end sequencing.

A total of 334 control cells, 425 extreme cells and 4 reference cells were whole-genome sequenced in three independent experiments. Of these, 730 samples (315 control cells, 412 extremes and 3 reference cells) met our minimal requirement of 10× coverage of 90% of the genome and did not exhibit strong fluctuations of the coverage. Seventy-five percent of the genome within the samples analysed had a mean coverage of 56× or higher. The raw data for all sequenced genomes are available at http://www.ebi.ac.uk/ena/data/view/PRJEB17891.

Genome alignment and variant calling. We set up a pipeline for determining genetic variants in yeast. More specifically, we aim to determine single nucleotide polymorphisms (SNPs), small insertion and deletions (indels), and structural variations (SVs). To that end we use the Illumina paired-end sequencing to sequence 100 bp and 125 bp, respectively, of both ends of each DNA fragment. After an initial quality control of the raw sequencing data (using FastQC, version 0.11.3, http://www.bioinformatics.babraham.ac.uk/projects/fastqc/) we trim adapters using cutadapt, version 1.8[32] and redo the quality control with FastQC. Then we align the read pairs using bwa-mem (version 0.7.12)[33] against an S288C (R64-1-1) reference sequence for *Saccharomyces cerevisiae*[34] and a reference sequence for *Saccharomyces paradoxus* (para2 from the Saccharomyces Genome Resequencing Project, ftp://ftp.sanger.ac.uk/pub/users/dmc/yeast/latest/misc.tgz). These alignments need further processing and thus we remove duplicates, sort, clean and index the alignments using the Picard tools (http://broadinstitute.github.io/picard/ version 2.4.1). We then check the read coverage of the reference genome using the Genome Analysis Toolkit (GATK, GenomeAnalysisTK-3.5) from the Broad Institute[35] and removed samples with insufficient coverage (less than 90% of the genome with coverage above 10×) or with unexpected strong fluctuating coverage. Mutations that were present in most sequenced samples were removed, as they correspond to constitutive variations between the reference genome and the founder cell, or mutations that arose early in the lineage and divided, as opposed to during the extreme event that was sorted for. We note that the vast majority of mutations removed this way were false positive; however, we did note a few cases in which mutation shared between the samples appeared real, perhaps indicating some ancestral relationship or positive contribution to fitness.

Defining SNPs and indels. For the discovery of *de novo* SNPs and indels, we run the HaplotypeCaller with parameter settings (-ploidy 1, -maxAltAlleles 1, -stand_call_conf 10, -stand_emit_conf 10) from GATK[36] on each sample, then collect all variants and rerun the HaplotypeCaller (HC) only on the predetermined loci ±150 bp (using the R packages GRanges[37] and VariantAnnotation[38] to collect the data) jointly on all samples (-ploidy 1, -maxAltAlleles 2, -stand_call_conf 10, -stand_emit_conf 10). We then scaled the minimal non-zero normalized, Phred-scaled genotype likelihoods (referred to as genotype quality) of each variant by the locus depth plus 0.25 × mean coverage and removed low coverage variants (local depth <10 and <20 specifically for telomeric regions due to their repetitive nature). For SNPs, we demanded a high depth-scaled genotype quality for the median of the reference calls and a depth-scaled genotype quality of at least 10. For indels, based on extensive Sanger validations, we set the threshold at a depth-scaled genotype quality of 10. Applying these stringent criteria retains high-quality variants with a presumably very low number of false positives, leads to a good performance with respect to all other quality metrics and ensures that at least ~60% of the reads covering the locus carry the alternative allele, the vast majority exhibiting more than 80% alternative reads (see Supplementary Information for details). We did not differentiate between repetitive and unique regions in our analysis; however, most of the loci with *de novo* variations had a mean mapping quality >50× indicating their location in a unique region of the genome. Finally, we used freebayes (version v0.9.21-7-g7dd41db[39]) to check whether we recover all of the SNPs determined by HC.

Defining SVs. To determine further structural variations, we applied a split read approach using the gapped alignment of reads (PINDEL[40], version 0.2.5b6) with parameter settings (--window_size 0.5, --max_range_index 4, --report_long_insertions true, --report_interchromosomal_events false), thus disabling the search for interchromosomal variants. A region from chromosome 12 exhibiting excessive coverage across samples was excluded from the search. The program reports on potential deletions, insertions, inversions and tandem duplications. As we are only interested in *de novo* mutations, we retain variants called in only one sample, and prefilter for those having on average a support of ≥4 unique reads per sample, with at least one left and right anchor read and a ratio of the number of supporting reads to the number of reference reads ≥0.1. A final filtering step keeps only those variants with more than 10 unique supporting reads. The maximum size of structural variations to be detected by this split read alignment is set to 8,092; however, only medium-size inserts up to a size of about 80 bp and 100 bp, respectively, can be detected as this is limited by the read size. To exploit the information from discordant mapped and split reads as reported by bwa mem we used LUMPY[41] (version 0.2.13). To obtain potential candidates, we require that there is support by more than five reads (split read or paired end), the relative support (support scaled by mean coverage of each sample) is larger than 5% and the fraction of the relative support is larger than 25%. The last requirement makes sure that the variants are only called in a small number of samples. As opposed to all other analysis we used SAMBLASTER[42] (version 0.1.22) to mark duplicates on untrimmed reads and to filter discordant and split alignments which are in turn fed into LUMPY.

In addition, we also applied a read-depth method analysing the number of read starts in windows of a size of 250 bp overlapping by 50 bp as determined by FREEC (version 7.0[43,44]). We normalize observed read counts per sample and per locus to remove corresponding biases and then filter on these normalized counts as well as demanding a size of 500 bp (loss of coverage) and 750 bp (gain of coverage), respectively, and a mean mappability larger than 0.75 to find genomic ranges with a gain or loss of coverage. For the determination of regions with an increase of coverage, we furthermore require the mean number of counts to be larger or equal to 60 and a separation of the observed signal from the background, and remove regions exhibiting a reciprocal overlap between different samples ≥50%. This was only necessary in experiments 1 and 2. This approach allows us effectively to determine ranges exhibiting a loss or gain of coverage with a size larger than about 0.5 to 1 kbp. Also, here we removed regions from chr8 and chr12 exhibiting excessive coverage (see Supplementary Information for details).

Detected SVs were visualized by plotting the normalized number of read counts in overlapping 250 bp windows alongside the lower and upper quartile of the background distribution of counts scaled by the median counts of the corresponding chromosome (grey). Read number is normalized by the local median chromosome scaled read counts. Repetitive sequences and genes flanking the mutated locus are shown with colour indicating orientation.

Testing for chromosome aneuploidy. We tested for chromosome aneuploidy, excluding the region from chr12 exhibiting excessive coverage, using samtools[45]

(version 1.2) and normalized copy number profiles inferred from the FREEC data. Cell ploidy was verified by DNA staining FACS analysis[46].

Defining mutation enrichment based on literature values. Considering a specific mutation type, occurring at a frequency p per nucleotide site, per division, the probability of not being mutated equals $1 - Ng\,p$, where Ng is the genome size. Consequently, the probability s to observe one or more mutations acquired during the 25 cell divisions before the single-cell bottleneck, is calculated as $s = 1 - (1 - Ng\,p)^{25}$. The probability of obtaining exactly N_m mutated samples from the total N_s characterized samples is given by the binomial distribution $B(N_s, N_m, s)$. We therefore perform a binomial test against the alternative hypothesis that the true probability to observe one or more mutations is greater than s based on literature estimates[25–27]. To directly compare the extreme and control samples, we perform a Fisher's exact test against the alternative that the odds ratio of mutated extreme versus mutated control samples is greater than 1, i.e. one sided P-values are reported. Please note that we classify a sample as being mutated if it carries at least one *de novo* mutation. For calculations of mutation rates in extreme and control cells refer to the Supplementary Information.

Data availability. All sequenced genomes are available at http://www.ebi.ac.uk/ena/data/view/PRJEB17891.

Received 7 September 2016; accepted 13 October 2016; published 4 January 2017

References

1. Bigger, J. Treatment of staphylococcal infections with penicillin by intermittent sterilisation. *Lancet* **244,** 497–500 (1944).
2. Maisonneuve, E. & Gerdes, K. Molecular mechanisms underlying bacterial persisters. *Cell* **157,** 539–548 (2014).
3. Lewis, K. Persister cells. *Annu. Rev. Microbiol.* **64,** 357–372 (2010).
4. Dhar, N. & McKinney, J. D. Microbial phenotypic heterogeneity and antibiotic tolerance. *Curr. Opin. Microbiol.* **10,** 30–38 (2007).
5. Gefen, O. & Balaban, N. Q. The importance of being persistent: heterogeneity of bacterial populations under antibiotic stress. *FEMS Microbiol. Rev.* **33,** 704–717 (2009).
6. Jayaraman, R. Bacterial persistence: some new insights into an old phenomenon. *J. Biosci.* **33,** 795–805 (2008).
7. Balaban, N. Q., Merrin, J., Chait, R., Kowalik, L. & Leibler, S. Bacterial persistence as a phenotypic switch. *Science* **305,** 1622–1625 (2004).
8. Balaban, N. Q. Persistence: mechanisms for triggering and enhancing phenotypic variability. *Curr. Opin. Genet. Dev.* **21,** 768–775 (2011).
9. Allison, K. R., Brynildsen, M. P. & Collins, J. J. Heterogeneous bacterial persisters and engineering approaches to eliminate them. *Curr. Opin. Microbiol.* **14,** 593–598 (2011).
10. Nathan, C. Fresh approaches to anti-infective therapies. *Sci. Trans. Med.* **4,** 140sr142 (2012).
11. Lewis, K. Persister cells, dormancy and infectious disease. *Nat. Rev. Microbiol.* **5,** 48–56 (2007).
12. Glickman, M. S. & Sawyers, C. L. Converting cancer therapies into cures: lessons from infectious diseases. *Cell* **148,** 1089–1098 (2012).
13. Knoechel, B. *et al.* An epigenetic mechanism of resistance to targeted therapy in T cell acute lymphoblastic leukemia. *Nat. Genet.* **46,** 364–370 (2014).
14. Welch, A. Z., Gibney, P. A., Botstein, D. & Koshland, D. E. TOR and RAS pathways regulate desiccation tolerance in *Saccharomyces cerevisiae*. *Mol. Biol. Cell* **24,** 115–128 (2013).
15. Levy, S. F., Ziv, N. & Siegal, M. L. Bet hedging in yeast by heterogeneous, age-correlated expression of a stress protectant. *PLoS Biol.* **10,** e1001325 (2012).
16. Stewart-Ornstein, J., Weissman, J. S. & El-Samad, H. Cellular noise regulons underlie fluctuations in *Saccharomyces cerevisiae*. *Mol. Cell* **45,** 483–493 (2012).
17. Gasch, A. P. *et al.* Genomic expression programs in the response of yeast cells to environmental changes. *Mol. Biol. Cell* **11,** 4241–4257 (2000).
18. Weinert, T. & Hartwell, L. Control of G2 delay by the *RAD9* gene of *Saccharomyces cerevisiae*. *J. Cell Sci. Suppl.* **12,** 145–148 (1989).
19. Weinert, T. A. & Hartwell, L. H. The *RAD9* gene controls the cell cycle response to DNA damage in *Saccharomyces cerevisiae*. *Science* **241,** 317–322 (1988).
20. Lisby, M., Rothstein, R. & Mortensen, U. H. Rad52 forms DNA repair and recombination centers during S phase. *Proc. Natl Acad. Sci. USA* **98,** 8276–8282 (2001).
21. Lisby, M., Mortensen, U. H. & Rothstein, R. Colocalization of multiple DNA double-strand breaks at a single Rad52 repair centre. *Nat. Cell Biol.* **5,** 572–577 (2003).
22. Domkin, V., Thelander, L. & Chabes, A. Yeast DNA damage-inducible Rnr3 has a very low catalytic activity strongly stimulated after the formation of a cross-talking Rnr1/Rnr3 complex. *J. Biol. Chem.* **277,** 18574–18578 (2002).
23. Hendry, J. A., Tan, G., Ou, J., Boone, C. & Brown, G. W. Leveraging DNA damage response signaling to identify yeast genes controlling genome stability. *G3* **5,** 997–1006 (2015).
24. Berry, D. B. & Gasch, A. P. Stress-activated genomic expression changes serve a preparative role for impending stress in yeast. *Mol. Biol. Cell* **19,** 4580–4587 (2008).
25. Lynch, M. *et al.* A genome-wide view of the spectrum of spontaneous mutations in yeast. *Proc. Natl Acad. Sci. USA* **105,** 9272–9277 (2008).
26. Nishant, K. T. *et al.* The baker's yeast diploid genome is remarkably stable in vegetative growth and meiosis. *PLoS Genet.* **6,** e1001109 (2010).
27. Serero, A., Jubin, C., Loeillet, S., Legoix-Ne, P. & Nicolas, A. G. Mutational landscape of yeast mutator strains. *Proc. Natl Acad. Sci. USA* **111,** 1897–1902 (2014).
28. Huh, W. K. *et al.* Global analysis of protein localization in budding yeast. *Nature* **425,** 686–691 (2003).
29. Janke, C. *et al.* A versatile toolbox for PCR-based tagging of yeast genes: new fluorescent proteins, more markers and promoter substitution cassettes. *Yeast* **21,** 947–962 (2004).
30. Lee, S. E. *et al.* Saccharomyces Ku70, mre11/rad50 and RPA proteins regulate adaptation to G2/M arrest after DNA damage. *Cell* **94,** 399–409 (1998).
31. Blecher-Gonen, R. *et al.* High-throughput chromatin immunoprecipitation for genome-wide mapping of in vivo protein-DNA interactions and epigenomic states. *Nat. Protoc.* **8,** 539–554 (2013).
32. Martin, M. Cutadapt removes adapter sequences from high-throughput sequencing reads. *EMBnet J.* **1,** 10–12 (2011).
33. Li, H. Aligning sequence reads, clone sequences and assembly contigs with BWA-MEM. Preprint at http://arXiv.org/abs/1303.3997v2 (2013).
34. Cherry, J. M. *et al.* Saccharomyces Genome Database: the genomics resource of budding yeast. *Nucleic Acids Res.* **40,** D700–D705 (2012).
35. McKenna, A. *et al.* The Genome Analysis Toolkit: a MapReduce framework for analyzing next-generation DNA sequencing data. *Genome Res.* **20,** 1297–1303 (2010).
36. DePristo, M. A. *et al.* A framework for variation discovery and genotyping using next-generation DNA sequencing data. *Nat. Genet.* **43,** 491–498 (2011).
37. Lawrence, M. *et al.* Software for computing and annotating genomic ranges. *PLoS Computat. Biol.* **9,** e1003118 (2013).
38. Obenchain, V. *et al.* VariantAnnotation: a Bioconductor package for exploration and annotation of genetic variants. *Bioinformatics* **30,** 2076–2078 (2014).
39. Garrison, E. & Marth, G. Haplotype-based variant detection from short-read sequencing. Preprint at http://arXiv.org/abs/1207.3907 (2012).
40. Ye, K., Schulz, M. H., Long, Q., Apweiler, R. & Ning, Z. Pindel: a pattern growth approach to detect break points of large deletions and medium sized insertions from paired-end short reads. *Bioinformatics* **25,** 2865–2871 (2009).
41. Layer, R. M., Chiang, C., Quinlan, A. R. & Hall, I. M. LUMPY: a probabilistic framework for structural variant discovery. *Genome Biol.* **15,** R84 (2014).
42. Faust, G. G. & Hall, I. M. SAMBLASTER: fast duplicate marking and structural variant read extraction. *Bioinformatics* **30,** 2503–2505 (2014).
43. Boeva, V. *et al.* Control-FREEC: a tool for assessing copy number and allelic content using next-generation sequencing data. *Bioinformatics* **28,** 423–425 (2012).
44. Boeva, V. *et al.* Control-free calling of copy number alterations in deep-sequencing data using GC-content normalization. *Bioinformatics* **27,** 268–269 (2011).
45. Li, H. *et al.* The Sequence Alignment/Map format and SAMtools. *Bioinformatics* **25,** 2078–2079 (2009).
46. Koren, A., Soifer, I. & Barkai, N. *MRC1*-dependent scaling of the budding yeast DNA replication timing program. *Genome Res.* **20,** 781–790 (2010).

Acknowledgements

We thank our group members for discussions and comments. We thank the Weizmann Institute of Science Flow Cytometry unit for support and O. Golani for help with the cell segmentation macro. This work was supported by the Minerva Center, European Research Council and the Israel Science Foundation. K.B. was supported by the European Molecular Biology Organization long-term fellowship.

Author contributions

All authors designed the study and analysed the results. G.Y., D.L. and J.S. performed the experiments; K.B. analysed the whole genome sequencing data. N.B., G.Y., D.L. and K.B. wrote the manuscript.

Additional information

Supplementary information is available for this paper.

Reprints and permissions information is available at www.nature.com/reprints.

Correspondence and requests for materials should be addressed to G.Y. and N.B.

How to cite this article: Yaakov, G., Lerner, D., Bentele, K., Steinberger, J. & Barkai, N. Coupling phenotypic persistence to DNA damage increases genetic diversity in severe stress. *Nat. Ecol. Evol.* **1,** 0016 (2017).

Competing interests

The authors declare no competing financial interests.